CH_2 revisited[1]

Apostolos Kalemos, Thom H. Dunning, Jr., Aristides Mavridis, and James F. Harrison

Abstract: The first four states of the CH_2 molecule ($\tilde{X}^3B_1$, $\tilde{a}^1A_1$, $\tilde{b}^1A_1$, and $\tilde{c}^1A_1$) are examined using state-of-the-art ab initio methods and basis sets. The construction of potential energy curves with respect to the C + H_2 and CH + H channels provides significant clues to understanding the geometric and electronic structure of the above states. All of our numerical findings are in excellent agreement with the existing experimental data.

Key words: CH_2, MRCI, potential curves, vbL icons.

Résumé : Les quatre premiers états électroniques de la molécule CH_2 ($\tilde{X}^3B_1$, $\tilde{a}^1A_1$, $\tilde{b}^1A_1$ et $\tilde{c}^1A_1$) ont été examinés en utilisant des méthodes ab initio et à l'aide des bases les plus étendues. Des courbes d'énergie potentielle par rapport aux C + H_2 et CH + H, nous donnent des renseignements importants pour la structure géométrique et électronique de ces états. Tous nos résultats sont en excellent accord avec les valeurs expérimentales.

Mots clés : CH_2, MRCI, courbes de potentiel, icônes vbL.

Introduction

The methylene molecule continues to be of interest to experimentalists and theoreticians alike (1–121) some 70 years after Mulliken's (1) pioneering theoretical work on its structure, and 60 years after Herzberg's (2) note on the 4050 group in cometary spectra. The reasons for this interest have been detailed in several reviews (8, 21, 27, 28, 65, 67, 70).

Methylene (CH_2) is: (*i*) the basic unit for divalent carbon chemistry, (*ii*) the smallest polyatomic radical with a ground triplet state and several low-lying singlets, (*iii*) a molecule with a remarkably complex electronic spectrum, and (*iv*) small enough to be studied by sophisticated ab initio methods. As discussed by Schaefer (70) the story of methylene is the story of the coming of age of computational quantum chemistry and, indeed, methylene has become a "paradigm for quantitative theoretical chemistry". We agree whole-heartedly with this assessment and in particular with the identification of the year 1970 as the origin of the coming of age (70). When one looks back on 1970 by citing the papers published during that year, one misses part of the excitement of the times, because much was going on in the background vis-à-vis preprints and personal communications. Some hint of this is found in the Herzberg and Johns 1971 paper (16) where the authors reinterpret the vacuum UV spectrum of methylene in terms of a bent structure of the radical. The acknowledgement in this paper reads "We are much indebted to Dr. Bernheim, Dr. Wasserman, Dr. Bender, and Dr. Harrison for sending us preprints of their papers." While both the Bernheim and Wasserman papers had appeared in print by the time the Herzberg and Johns paper was published, the referenced preprints of Bender and Harrison had not. From an historical perspective it is interesting to revisit the activities of 1970 by looking at the submission dates of the various CH_2-related papers.

The first of the 1970 papers was submitted in May by Bernheim et al. (10), and was the opening salvo that something might be wrong with the widely held belief that the ground triplet state of CH_2 was linear. On the basis of ESR measurements these authors suggested that the ground state of CH_2 was indeed a triplet and was slightly bent in a xenon matrix at 4.2 K.

A few weeks later the manuscript by Bender and Schaefer (9) was received and these authors explicitly challenged experiment, declaring that "... on the basis of the present and

Received 3 November 2003. Published on the NRC Research Press Web site at http://canjchem.nrc.ca on 14 June 2004.

A. Kalemos and T.H. Dunning, Jr.[2] Joint Institute for Computational Sciences, University of Tennessee, Oak Ridge National Laboratory, 1 Bethel Valley Road, Oak Ridge, TN 37831–6008, USA; Department of Chemistry, University of Tennessee, Knoxville, TN 37996–1600, USA; Computer Science and Mathematics Division, Oak Ridge National Laboratory, Oak Ridge, TN 37831–6008, USA.
A. Mavridis. Laboratory of Physical Chemistry, Department of Chemistry, National and Kapodistrian University of Athens, PO Box 64004, 157 10 Zografou, Athens, Greece.
J.F. Harrison. Department of Chemistry and Center for Fundamental Materials Research, Michigan State University, East Lansing, MI 48824–1322, USA.

[1]This article is part of a Special Issue dedicated to the memory of Professor Gerhard Herzberg.
[2]Corresponding author (e-mail: dunningthjr@ornl.gov).

 doi: 10.1139/V04-045

previous ab initio calculations and the stated numerical uncertainties, we conclude that the CH_2 ground state is nonlinear with a geometry close to r = 1.096 Å, θ = 135.1°." The previous ab initio calculations referred to were those of Foster and Boys (4) and Harrison and Allen (8).

In the ensuing month of July 1970, Harrison (13) submitted a manuscript describing an ab initio calculation of the angular dependence of the zero-field splitting (ZFS) parameters (D and E) of CH_2. If one could compare the computed D, and, in particular the E parameter, to the experimental, one could provide additional evidence for the CH_2 bond angle. In the course of these calculations the bond angle of CH_2 in the $\tilde{X}^3B_1$ state was computed to be 132.5°. Noting the disagreement with Herzberg and theoretical predictions, Harrison stated: "It seems that this persistent discrepancy between theory and experiment warrants a critical evaluation of the experimental data." This was the second formal challenge, following Bender and Schaefer (9), to the accepted view that CH_2 was linear.

August passed uneventfully and in September Wasserman et al. (11) submitted a manuscript in which they challenged the status quo by suggesting that CH_2 has a bond angle of 136°, in good agreement with the theoretical values (9, 13).

October saw two submissions. The first was a theoretical study by O'Neil et al. (20) in which they calculated potential energy surfaces for seven electronic states of CH_2, and an experimental ESR study of CH_2, CD_2, and CHD by Wasserman et al. (12), who concluded that the ground triplet state of CH_2 is bent with an angle of 136°.

In November, Harrison (14) submitted a second paper focused on the geometry and electronic structure of CH_2, CHF, and CF_2 and concluded again that the CH_2 $\tilde{X}^3B_1$ angle was 132.5°.

In the following month of December 1970, Herzberg and Johns (16) submitted their reinterpretation of the CH_2 angle and noted: "The considerations given here point strongly toward the bent structure of the triplet ground ($\tilde{X}^3B_1$) state of CH_2, as suggested by the electron-spin resonance work and the ab initio calculations."

Soon afterwards three important experimental ESR papers appeared. The first was titled "^{13}C Hyperfine Interactions in CD_2" by Bernheim et al. (17), (received on 11 January 1971), concluding that the CH_2 angle was 137.7°. The second was titled "^{13}C Hyperfine Interactions and Geometry of Methylene" by Wasserman et al. (18), (received in February 1971) concluding that the angle was 136 ± 5°. The third was also from the Wasserman group (19), "Zero-Field Parameters of Free CH_2; Spin-Orbit Contributions in Xenon" (received on 14 June 1971). This report concluded that the xenon matrix has a large effect on the observed zero-field parameters of CH_2 via intermolecular spin-orbit interactions and once this is accounted for, the experimental ZFS parameters were in good agreement with the calculations of Harrison (13).

The second problem of great importance with methylene was the singlet-triplet splitting ($\tilde{a}^1A_1 \leftarrow \tilde{X}^3B_1$) and this was resolved over a longer period of time and has been discussed in the excellent reviews of Shavitt (65), Goddard (67), and Schaefer (70).

In spite of the phenomenal interest in the CH_2 molecule, truly definitive calculations on other than the lowest $\tilde{X}^3B_1$ and $\tilde{a}^1A_1$ states are rare. It is our intention to study the electronic and geometric structure of the ground and excited states of CH_2 as accurately as conventional theory will permit. To this end, we report on the first four states of CH_2 ($\tilde{X}^3B_1$, $\tilde{a}^1A_1$, $\tilde{b}^1B_1$, and $\tilde{c}^1A_1$) employing all-electron variational multireference calculations in conjunction with very large basis sets. For all states above, potential energy profiles were constructed with respect to the HĈH (= θ) angle, and to the $CH_2 \rightarrow CH + H$ channel. We believe that our interpretation, coupled with our consistent numerical results, offers a fresh view in the conceptual saga of the CH_2 molecule.

Methodology and insights

For the C atom, the doubly augmented correlation consistent polarized core-valence basis set of sextuple quality (d-aug-cc-pCV6Z, 22*s*16*p*10*d*9*f*6*g*4*h*2*i*) of Dunning and coworkers (122) was employed. The core set was that of quintuple quality basis (i.e., 4*s*4*p*3*d*2*f*1*g*). For the H atom the plain sextuple cc-basis set (10*s*5*p*4*d*3*f*2*g*1*h*) was used (123).[3] Both were generally contracted to [13*s*12*p*10*d*8*f*6*g*4*h*2*i*/$_C$ 6*s*5*p*4*d*3*f*2*g*1*h*/$_H$] resulting in 461 spherical Gaussian functions. The spherically averaged SCF energy of the ^{3}P ground state of the C atom using the above basis set is –37.688 612 E_h, just 7 μE_h above the numerical value (124).

The method of choice followed in the present work is the standard internally contracted multireference CISD, based on a full valence (2*s* + 2*p* on C and 1*s* on Hs) complete active SCF zero order wave function (CASSCF). By distributing the six valence (active) electrons in the six orbitals, the CASSCF wave functions obtained contain 51, 56, 39, and 56 configuration functions (CF) for the $\tilde{X}^3B_1$, $\tilde{a}^1A_1$, $\tilde{b}^1A_1$, and $\tilde{c}^1A_1$ states, respectively.

The CI expansion is generated by single and double replacements of all eight electrons (the ~$1s^2$ e^- of C included) out of the reference space (CASSCF(6e^-/6 orbitals) + 1 + 2 = MRCI(8e^-)) within the internally contracted ansatz as implemented in the MOLPRO package (125). The uncontracted MRCI expansions comprise 27.5 × 10^6 ($\tilde{X}^3B_1$), 18.3 × 10^6 ($\tilde{a}^1A_1$, $\tilde{c}^1A_1$), 15.9 × 10^6 ($\tilde{b}^1B_1$) CFs, reduced to about 1.3 × 10^6 CFs in the internally contracted approximation.

Due to the extended basis sets used no corrections for basis set superposition errors (BSSE) were considered. Size non-extensivity errors are reasonably small: at the MRCI level non-extensivity with respect to C(^{3}P; ^{1}D) + $H_2(X^1\sum_g^+)$ amounts to 1.59, 1.43, 1.42, and 1.42 mE_h for the $\tilde{X}^3B_1$,

[3] Basis sets were obtained from the Extensible computational chemistry environment basis set database, version 6/19/03, as developed and distributed by the Molecular Science Computing Facility, Environmental and Molecular Sciences Laboratory which is part of the Pacific Northwest Laboratory, PO Box 999, Richland, Washington 99352, USA, and funded by the US Department of Energy. The Pacific Northwest Laboratory is a multiprogram laboratory operated by Battelle Memorial Institute for the US Department of Energy under contract DE–AC06–76RLO 1830. Contact David Feller or Karen Schuchardt for further information.

Fig. 1. Potential energy profiles of the $\tilde{X}^3B_1$, $\tilde{a}^1A_1$, $\tilde{b}^1B_1$, and $\tilde{c}^1A_1$ CH_2 states at the all-electron MRCI level along the HĈH bending mode.

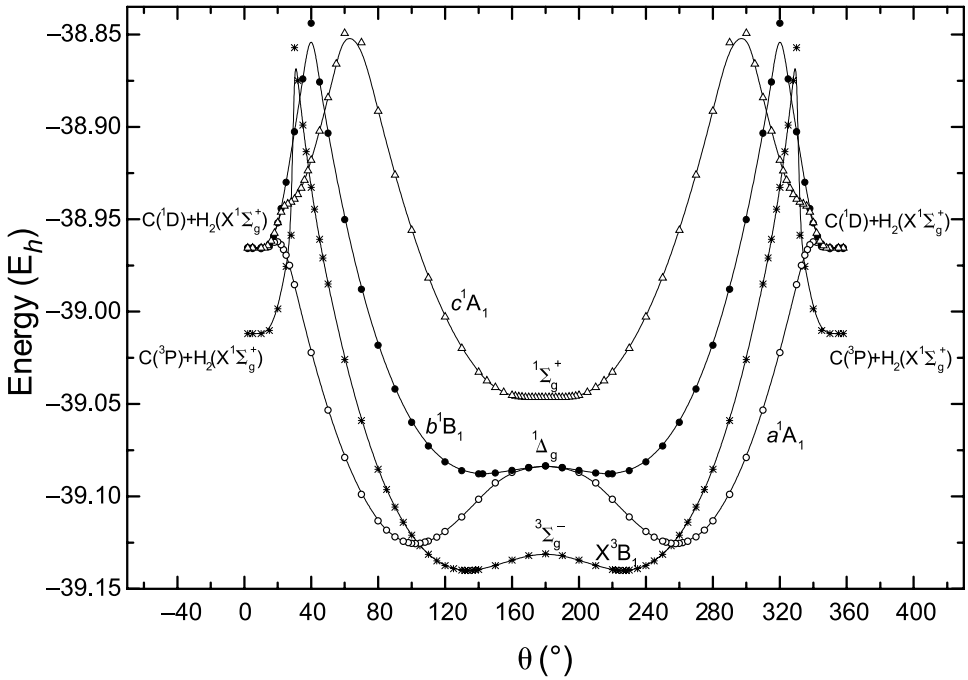

$\tilde{a}^1A_1$, $\tilde{b}^1B_1$, and $\tilde{c}^1A_1$ states, respectively. Restricted coupled cluster singles and doubles with perturbative triples computations (RCCSD(T)) were also performed for the $\tilde{X}^3B_1$ state around the equilibrium geometry.

For the first four states of the CH_2 molecule studied in the present work ($\tilde{X}^3B_1$, $\tilde{a}^1A_1$, $\tilde{b}^1B_1$, and $\tilde{c}^1A_1$) in ascending energy order, two obvious channels of formation can be considered, C + H_2 → CH_2 or H + CH → CH_2. In detail,

[1*a*] $CH_2(\tilde{X}^3B_1) \xrightarrow{C_{2v}} C(2p_z^1 2p_x^1; {}^3P) + H_2(X^1\Sigma_g^+)$

↓

[1*b*] $HCH(^3\Sigma_g^-) \xrightarrow{C_{\infty v}} CH(a^4\Sigma^-) + H(^2S)$

[2*a*] $HCH(^1\Delta_g) \xrightarrow{C_{2v}} CH_2(\tilde{a}^1A_1) \xrightarrow{C_{2v}}$

$C[1/\sqrt{2}(2p_z^2 - 2p_y^2); {}^1D] + H_2(X^1\Sigma_g^+) \xrightarrow{C_{2v}}$

$CH_2(\tilde{b}^1B_1) \xrightarrow{C_{2v}} C(2p_z^1 2\bar{p}_x^1; {}^1D) + H_2(X^1\Sigma_g^+)$

↓

[2*b*] $\xrightarrow{C_{\infty v}} CH(A^2\Delta) + H(^2S)$

[3*a*] $CH_2(\tilde{c}^1A_1) \xrightarrow{C_{2v}} C\{1/\sqrt{6}[2(2p_z^2) - 2p_x^2 - 2p_y^2]; {}^1D\} + H_2(X^1\Sigma_g^+)$

↓

[3*b*] $HCH(^1\Sigma_g^+) \xrightarrow{C_{\infty v}} CH(C^2\Sigma^+) + H(^2S)$

Two sets of fully optimized potential energy curves have been constructed at the all-electron MRCI level; one along the bending coordinate HĈH = θ (eqs. [1*a*], [2*a*], and [3*a*]), and a second one along the asymmetric CH + H dissociation mode (eqs. [1*b*], [2*b*], and [3*b*]) (Figs. 1 and 2). For the first set of curves, the C—H bond distance was optimized for each angle (HĈH); for the second set of curves HĈH = 180° and the C—H bond distances were optimized for each HC-H separation.

Results and discussion

Table 1 lists the most recent and reliable theoretical and experimental results of the literature on the first four states of the CH_2 carbene pertaining to the present work, while Tables 2 and 3 refer to this work. Figures 1 and 2 depict potential energy curves with respect to the HĈH = θ angle (eqs. [1*a*], [2*a*], and [3*a*]) and to the HCH → CH + H dissociation channel (eqs. [1*b*], [2*b*], and [3*b*]).

$\tilde{X}^3B_1$

The leading CASSCF configuration is

$$\left|\tilde{X}^3B_1\right\rangle \sim 0.99\left|1a_1^2\ 2a_1^2 3a_1^1\ 1b_1^1\ 1b_2^2\right\rangle$$

where $1a_1 \sim 1s_C$, $2a_1 \sim 0.79(2s)_C + 0.20(2p_z)_C + 0.73(1s_A + 1s_B)_H$, $3a_1 \sim 0.38(2s)_C - 0.85(2p_z)_C - 0.29(1s_A + 1s_B)_H$, $1b_1 \sim (2p_x)_C$, $1b_2 \sim 0.70(2p_y)_C + 0.93(1s_A - 1s_B)_H$ with corresponding CASSCF atomic Mulliken populations (C/H) ($1s^{2.0}2s^{1.38}2p_z^{0.90}2p_x^{0.98}2p_y^{1.03}/1s^{0.80}2p^{0.03}$).

The analogous distributions of the $a^4\Sigma^-$ CH diatomic at the same level of theory are ($1s^{2.0}2s^{1.42}2p_z^{0.71}2p_x^{0.98}2p_y^{0.98}$/ $1s^{0.72}2p^{0.03}$), indicating clearly the common ancestry of both species to the $^5S(2s^12p^3)$ atomic state of carbon atom.

The valence-bond Lewis (vbL) diagram of the parental CH $a^4\Sigma^-$ state (see also ref. 126)

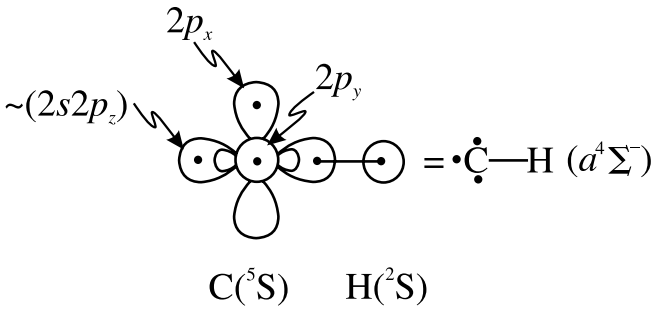

suggests two modes of attack of the second H(^{2}S) atom to form CH_2, linear and perpendicular, (i.e., along the z and x (or y) axes) predicting in turn a linear ($^3\Sigma_g^-$) or a bent ($^3B_1(\theta = 90°)$) CH_2 ground state, respectively. Diagrammatically,

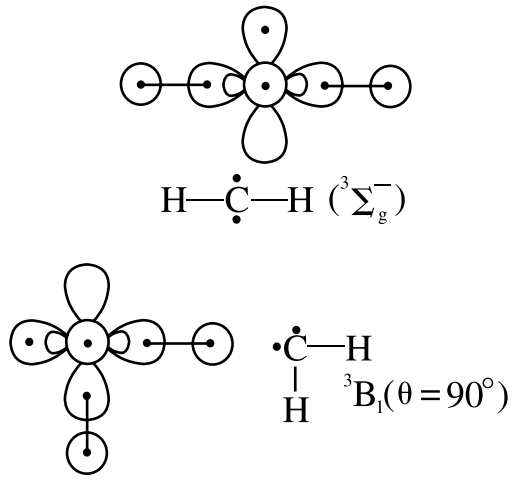

The binding energy with respect to CH($a^4\Sigma^-$) + H(^{2}S) of the $^3\Sigma_g^-$ configuration is 116.5 kcal/mol (Fig. 2), 15.9 kcal/mol *higher* than that of the bent structure at θ = 90°. The equilibrium geometry is determined by the differences in energy between binding to the ($2s$–$\lambda 2p_z$) orbital and the $2p_x$ orbital, which favors a bond angle less than 180°, and the repulsion between the CH bond pairs, which favors a bond angle greater than 90°. This may also be viewed as the vibronic interaction of the two limiting $^3\Sigma_g^-$ and $^3B_1(\theta = 90°)$ structures through a pseudo Jahn–Teller effect. The result is a final bent geometry of θ_e = 133.66° (Table 2). Remarkably enough, the arithmetic average of the angles of the two limiting structures is (180° + 90°)/2 = 135°. This analysis supports a rather low inversion barrier, which, indeed, according to our calculations is just 1982.5 cm^{-1} (= 5.668 kcal/mol).

Our geometrical results (r_e, θ_e) are in complete agreement with the most recent theoretical results of Császár et al. (121), and in excellent agreement with existing experimental numbers (Tables 1 and 2) in both RCCSD(T) and MRCI methodologies. Our predicted atomization energy (AE_e) at the RCCSD(T)[MRCI+Q] level of theory is 190.06 [189.9] kcal/mol, as compared to a mixed experimental (AE_0) (127) plus theoretical (ZPE) (121) value of AE_e = AE_0 + ZPE = 180.043 + 10.683 = 190.73 kcal/mol.

Fig. 2. Potential energy profiles of the CH + H channel at the all-electron MRCI level.

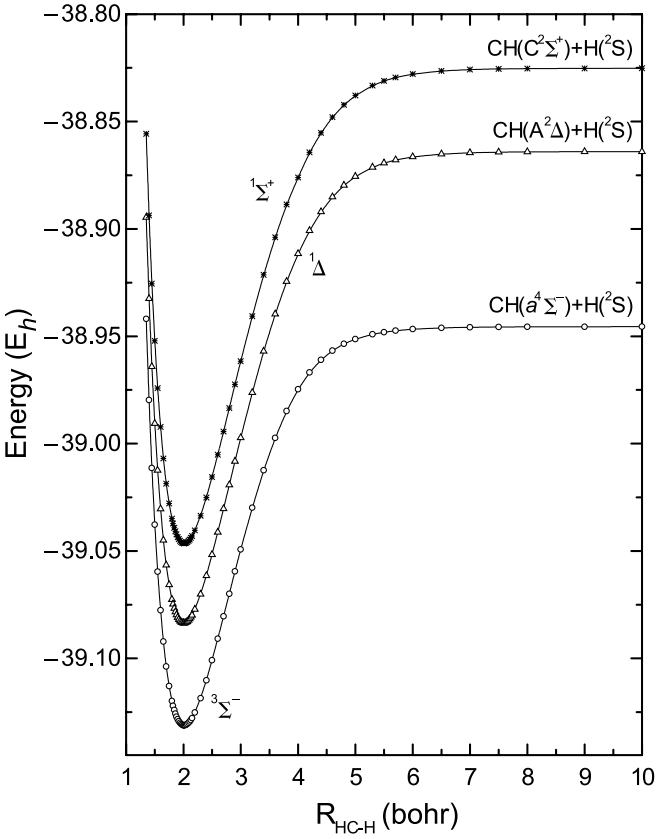

$\tilde{a}^1A_1$

The two most important configurations of the $\tilde{a}^1A_1$ state (CASSCF) are

$$\left|\tilde{a}^1A_1\right\rangle \sim \left|1a_1^2\ 2a_1^2[0.97(3a_1^2) - 0.21(1b_1^2)]1b_2^2\right\rangle$$

where the "0.21" contribution is a symmetry dictated determinant (at the linear configuration). This configuration can also be viewed as a GVB angular correlation term arising from the $2s$–$2p$ near degeneracy in the carbon atom. At θ = 180° the $\tilde{a}^1A_1$ state of CH_2 correlates to the linear $^1\Delta_g$ symmetry (Fig. 1). Returning now to the low-lying states of the CH diatomic (126), it is observed that the linear $^1\Delta_g$ structure correlates to the CH($A^2\Delta$) + H(^{2}S) fragments (Fig. 2), while the bent structure ($^1A_1$) emanates from the $X^2\Pi$ state of CH, 67.46 kcal/mol *below* the $A^2\Delta$ state (Table 3). Pictorially, the two CH states can be represented as follows (126): Mutatis mutandis with the $\tilde{X}^3B_1$ discussion, a linear and perpendicular H attack on the $A^2\Delta$ and $X^2\Pi$ states of CH is pos-

Table 1. Recent ("best") theoretical and experimental results on the $\tilde{X}^3B_1$, $\tilde{a}^1A_1$, $\tilde{b}^1B_1$, and $\tilde{c}^1A_1$ states of CH_2.

$-E$ (hartree)	r_e (Å)	θ_e (°)	ZPE (cm^{-1})	T_e/T_0 (kcal/mol)	Reference (year)
$\tilde{X}^3B_1$					
39.0911477[a]	1.075981	133.8483		0.0	121 (2003)
39.1469003[b]	1.075981	133.8483	3736.4[c]	0.0	121 (2003)
39.089879[d]	1.0767	133.56		0.0	101 (1995)
39.145107[e]	1.0751	133.79		0.0	101 (1995)
39.086206[f]	1.0769	133.51		0.0	101 (1995)
39.139165[g]	1.0750	133.70		0.0	101 (1995)
39.0830835[h]	1.079441	133.576	3715	0.0	84 (1989)
Expt.[i]	1.07530	133.9308	3689	0.0	82 (1988)
$\tilde{a}^1A_1$					
39.0764083[a]	1.106907	102.1369		9.249	121 (2003)
39.1315040[b]	1.106907	102.1369	3612.0	9.661 (9.306)	121 (2003)
				9.327 (8.972)[j]	121 (2003)
	1.099[k]	104	3621	9.192	117 (2000)
39.061054[l]	1.1102	101.72	3639.55	10.007 (9.548)	110 (1997)
39.072067[f,m]	1.1083	102.02		8.872	101 (1995)
39.124334[g,m]	1.1061	102.18		9.307	101 (1995)
Expt.[n]	1.107±0.002	102.4±0.4			85 (1989)
Expt.[i]				(8.998±0.014)	82 (1988)
$\tilde{b}^1B_1$					
	1.062[k,o]	144	4034.034	31.897 (32.883)	117 (2000)
39.022514[l]	1.0754	142.60	3764.41	34.191 (34.089)	110 (1997)
				(32.911±0.014)[p]	82 (1998), 112 (1998)
Expt.[q]	1.086	139.3			81 (1988)
Expt.[q]	1.053	140±15			7 (1966)
$\tilde{c}^1A_1$					
39.981153[l]	1.0683	171.34	3676.97	60.146 (59.794)	110 (1997)
38.985644[r]	1.067616	172.70	3923.2	59.513	105 (1996)
38.979005[s]	1.1063897	171.62	3970.5	60.271	104 (1996)

Note: Total energies (E), bond distances (r_e), HĈH angles (θ_e), zero point energies (ZPE), and energy gaps (T_e/T_0).

[a]RCCSD(T)/aug–cc–pCV6Z//RCCSD(T)/aug–cc–pCVQZ (valence electron calculation).

[b]RCCSD(T)/aug–cc–pCV6Z//RCCSD(T)/aug–cc–pCVQZ (all electron calculation).

[c]RCCSD(T)/aug–cc–pCVQZ level employing the nonrigid – rotation – large – amplitude internal motion Hamiltonian (NRLH) and quartic force fields.

[d]RCCSD(T)/cc–pCV5Z (valence electron calculation).

[e]RCCSD(T)/cc–pCV5Z (all electron calculation).

[f]MRCI/cc–pCV5Z (valence electron calculation).

[g]MRCI/cc–pCV5Z (all electron calculation).

[h]MORBID analysis on a MRCI/[5*s*4*p*3*d*2*f*1*g*/3*s*2*p*1*d*] energy surface.

[i]MORBID analysis on experimental data. Inversion barrier ($^3\Sigma_g^- \leftarrow \tilde{X}^3B_1$), IB = 1952 cm^{-1} at r_{CH} = 1.064 Å.

[j]Based on a focal point analysis corrected for core-correlation, relativistic, and adiabatic effects; the exact numbers given in ref. 121 are $9.327^{+0.083}_{-0.046}$ ($8.972^{+0.097}_{-0.069}$) kcal/mol.

[k]MORBID analysis on an ab initio (ref. 84; MRCI/[5*s*4*p*3*d*2*f*1*g*/3*s*2*p*1*d*]) surface that takes into account the Renner–Teller effect, and refined by fitting to the experimentally available vibrational term values. Inversion barrier ($^1\Delta_g \leftarrow \tilde{a}^1A_1$), IB = 8666.1 cm^{-1} at r_{CH} = 1.051 Å.

[l]MRCI/[6*s*4*p*2*d*1*f*/4*s*2*p*1*d*] with the $1s^2$ e^- frozen and the corresponding virtual orbital deleted. ZPE based on harmonic frequencies.

[m]RCCSD(T) and all e^- RCCSD(T) energies, –39.075 244 and –39.129 825 E_h, respectively.

[n]IR – flash – kinetic spectroscopy.

[o]Inversion barrier ($^1\Delta_g \leftarrow \tilde{b}^1B_1$), IB = 725.1 cm^{-1}.

[p]Based on the $\tilde{a}^1A_1 \leftarrow \tilde{X}^3B_1$ T_0 = 8.998 ± 0.014 kcal/mol splitting (ref. 82) and the $\tilde{b}^1B_1 \leftarrow \tilde{a}^1A_1$ T_0 = 8363.8 cm^{-1} = 23.913 kcal/mol (ref. 107) according to the stretch-bender (SB) Hamiltonian.

[q]r_0 and θ_0 values.

[r]MORBID analysis on a MRCI/[7*s*5*p*3*d*2*f*/5*s*3*p*2*d*] surface with the $1s^2$ e^- frozen and the corresponding virtual orbital removed. Inversion barrier ($^1\Sigma_g^+ \leftarrow \tilde{c}^1A_1$), IB = 6 cm^{-1}.

[s]MORBID analysis on a TC–CISD/[7*s*5*p*3*d*2*f*/5*s*3*p*2*d*] surface with the $1s^2$ e^- frozen and the corresponding virtual orbital removed. Inversion barrier ($^1\Sigma_g^+ \leftarrow \tilde{c}^1A_1$), IB = 12 cm^{-1}.

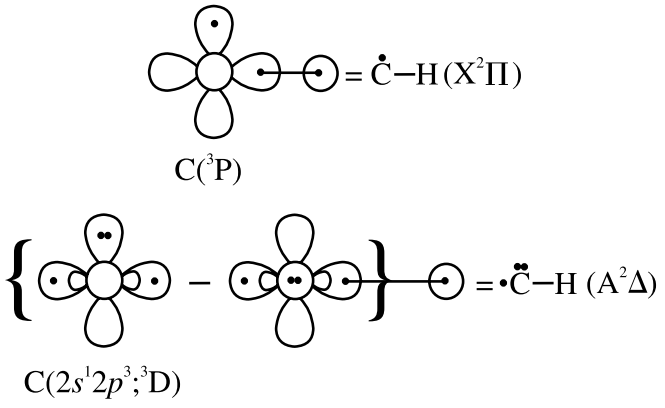

sible, resulting in the $^1\Delta_g$ and $^1A_1(\theta = 90°)$ symmetries of CH_2, or using the vbL iconal language,

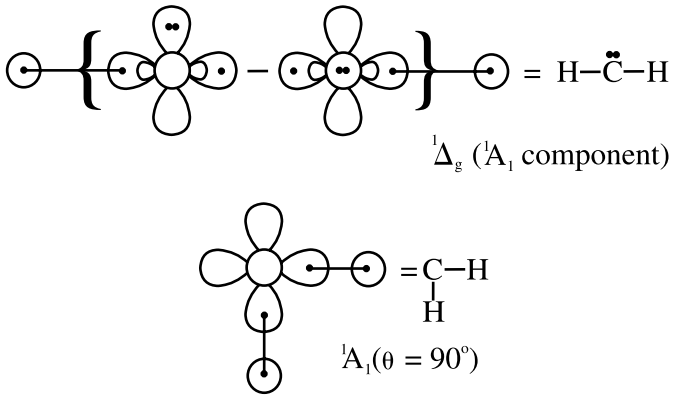

The CH-H binding energies are 94.42 kcal/mol with respect to $CH(X^2\Pi) + H(^2S)$, and 137.77 kcal/mol with respect to $CH(A^2)) + H(^2S)$ for the $^1A_1(\theta = 90°)$ and $^1\Delta_g$ symmetries, respectively (Fig. 2). The linear $^1\Delta_g$ configuration is stabilized by 137.77 – T_e(CH; $A^2\Delta \leftarrow X^2\Pi$) = 137.77 – 67.46 = 70.31 kcal/mol with respect to the ground CH state. Therefore, the bent $^1A_1(\theta = 90°)$ structure of CH_2 is favoured by 94.42 – 70.31 = 24.11 kcal/mol and mildly "relaxed" to a final angle of 102.20° ($\tilde{a}^1A_1$); see Table 2. The high energy inversion barrier of this state corresponds to the energy difference of the two limiting structures ($^1\Delta_g$, $^1A_1(\theta = 90°)$) increased by the relaxation energy $^1A_1(\theta = 90°) \rightarrow \tilde{a}^1A_1$ (θ_e = 102.20°) or IB = 67.46 – 43.35 + 2.24 = 26.35 kcal/mol (Table 2).

The geometrical values (r_e, θ_e) of Table 2 are in complete agreement with the focal point analysis of ref. 121. The $\tilde{a}^1A_1 \leftarrow \tilde{X}^3B_1$ splitting corrected for ZPE from ref. 121 is 8.822 kcal/mol as contrasted to the most recent experimental value of 8.998 ± 0.014 kcal/mol (82).

$\tilde{b}^1B_1$

The CASSCF main configuration for the $\tilde{b}^1B_1$ state is

$$\left|\tilde{b}^1B_1\right\rangle \sim 0.99 \left|1a_1^2\, 2a_1^2 3a_1^1 1\bar{b}_1^1 1b_2^2\right\rangle$$

As can be seen, this state is the open-shell singlet analog of the $\tilde{X}^3B_1$ state. As expected, the $\tilde{b}^1B_1$ molecular orbitals and Mulliken atomic distributions are very similar to those of the ground state (vide supra).

At linearity the symmetry of this state is $^1\Delta_g$; it is the Renner–Teller companion of the previously discussed $\tilde{a}^1A_1$ state (Fig. 1). The $A^2\Delta$ and $B^2\Sigma^-$ states of the diatomic CH molecule, differing in energy by 7.21 kcal/mol (Table 3), can be considered as the parental states of the $CH^2\tilde{b}\,^1B_1$ state. This is clearly seen from the following vbL diagrams:

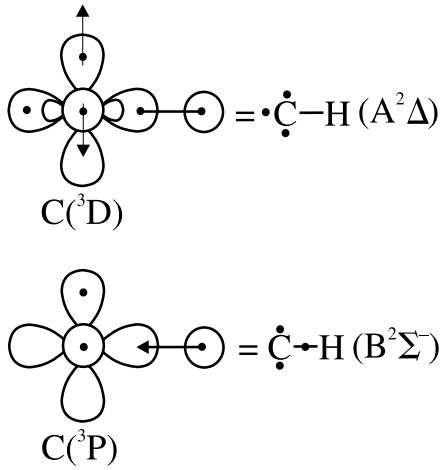

Two modes of H attack resulting in the formation of CH_2 are conceivable: a linear attack on the $A^2\Delta$ state of CH along the z axis and a perpendicular attack on the $B^2\Sigma^-$ state along the x (or y) axis, giving rise to $^1\Delta_g$ and $^1B_1(\theta = 90°)$ CH_2 symmetries, respectively. Diagrammatically,

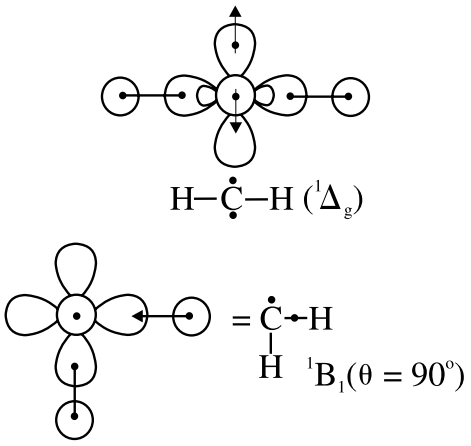

The binding energies of the $^1\Delta_g$ and $^1B_1(\theta = 90°)$ CH_2 configurations with respect to $CH(A^2\Delta$ or $B^2\Sigma^-) + H(^2S)$ are 137.77 and 118.86 kcal/mol, respectively (Fig. 2, Table 3). Therefore, the $^1\Delta_g$ structure is *lower* in energy by 137.77 – 118.86 + 7.21 = 26.12 kcal/mol. The pseudo Jahn–Teller interaction between the two limiting cases ($^1\Delta_g$ and $^1B_1(\theta = 90°)$) results in the $\tilde{b}^1B_1$ state with a final θ_e angle of 142.44° (Table 2), again very close to (180° + 90°)/2 = 135°. It is clear by now that everything else being equal, the inversion barrier is strongly related to the energy separation of the CH states involved, i.e., the relative low IB = 2.72 kcal/mol (Table 2) of the $\tilde{b}^1B_1$ state is related to the small CH $A^2\Delta \leftarrow B^2\Sigma^-$ splitting.

Our predicted $\tilde{b}^1B_1 \leftarrow \tilde{X}^3B_1$ separation is T_e =

Table 2. Total energies (E), equilibrium bond distances (r_e), HĈH angles (θ_e), dipole moments (μ_e), inversion barriers (IB), atomization energies (AE_e), and energy gaps (T_e/T_0) of the $\tilde{X}^3B_1$, $\tilde{a}^1A_1$, $\tilde{b}^1B_1$, and $\tilde{c}^1A_1$ states of CH_2.

$-E$ (hartree)	r_e (Å)	θ_e (°)	μ_e[a] (Debye)	IB (cm^{-1})	AE_e (kcal/mol)	T_e/T_0 (kcal/mol)
$\tilde{X}^3B_1$						
39.140113[b]	1.0751	133.66	0.596	1982.5[c]	188.90[d]	0.0
39.146232[e]	1.0753	133.82			190.06[f]	0.0
$\tilde{a}^1A_1$						
39.125487[b,g]	1.1061	102.20	1.676	9217.7[h]	179.72[i]	9.178/8.822[j]
$\tilde{b}^1B_1$						
39.087831[b,k]	1.0723	142.44	0.664	953.2[h]	156.09[i]	32.807/33.658[l]
$\tilde{c}^1A_1$						
39.046391[b,m]	1.0657	171.92	0.193	10.3[n]	130.09[i]	58.811/59.345[o]

Note: For the present work.
[a]Calculated as expectation value.
[b]All electron MRCI/[13s12p10d8f6g4h2i/6s5p4d3f2g1h]. E (+Q = Davidson correction) = –39.1464 E_h.
[c]IB = 1982.5 cm^{-1} (= 5.668 kcal/mol) at $r_{CH}(^3\Sigma_g^-)$ = 1.0648 Å.
[d]AE_e = IB + D_e[HCH($^3\Sigma_g^-$) → CH($a^4\Sigma^-$) + H(^{2}S)] + D_e[CH($a^4\Sigma^-$)] = 5.668 + 116.47 + 66.76 = 188.90 kcal/mol. At the MRCI + Q level, AE = 189.9 kcal/mol.
[e]All electron RCCSD(T).
[f]AE_e[$CH_2(\tilde{X}^3B_1)$ → C(^{3}P) + 2H(^{2}S)] = (39.146232 – 37.843350 – (2 × 0.4999992)) × 627.51 = 190.06 kcal/mol.
[g]E(+Q) = –39.1321 E_h.
[h]IB to linearity at $r_{CH}(^1\Delta_g)$ = 1.0622 Å.
[i]With respect to C(^{3}P) + 2H(^{2}S).
[j]$T_0(\tilde{a}^1A_1) = T_e(\tilde{a}^1A_1)$ – [ZPE($\tilde{X}^3B_1$) – ZPE($\tilde{a}^1A_1$)], with ZPEs from ref. 121 (see Table 1).
[k]E(+Q) = –39.0958 E_h.
[l]$T_0(\tilde{b}^1B_1) = T_e(\tilde{b}^1B_1)$ – [ZPE($\tilde{X}^3B_1$) – ZPE($\tilde{b}^1B_1$)], with ZPE($\tilde{X}^3B_1$) and ZPE($\tilde{b}^1B_1$) from refs. 121 and 117, respectively (see Table 1).
[m]E(+Q) = –39.0550 E_h.
[n]IB to linearity at $r_{CH}(^1\Sigma_g^+)$ = 1.0650 Å.
[o]$T_0(\tilde{c}^1A_1) = T_e(\tilde{c}^1A_1)$ – [ZPE($\tilde{X}^3B_1$) – ZPE($\tilde{c}^1A_1$)], with ZPE($\tilde{X}^3B_1$) and ZPE($\tilde{c}^1A_1$) from refs. 121 and 105, respectively (see Table 1).

Table 3. Total energies (E), bond distances (r_e), and energy separations (T_e) of the first five CH states at the all-electron MRCI/(d–aug–cc–pCV6Z/cc–pV6Z) level.

State	$-E$ (hartree)	r_e (Å)	T_e (kcal/mol)
$X^2\Pi$	38.471454	1.1179	0
		(1.119786)	(0)
$a^4\Sigma^-$	38.445470	1.0857	16.31
		(1.0977)[a]	(17.11±0.18)[a]
$A^2\Delta$	38.363946	1.1027	67.46
		(1.1031)	(66.19)
$B^2\Sigma^-$	38.352464	1.1719	74.67
		(1.1640)	(74.51)
$C^2\Sigma^+$	38.325164	1.1129	91.80
		(1.1143)	(90.93)

Note: From the present work; experimental values in parentheses (taken from ref. 126).
[a]r_0 and T_0 values.

32.807 kcal/mol, in excellent agreement with the best available experimental/theoretical value of 32.911 ± 0.014 kcal/mol (Tables 1 and 2).

$\tilde{c}^1A_1$

This is the highest energy state examined in the present report with a $\tilde{c}^1A_1 \leftarrow \tilde{X}^3B_1$ splitting T_e (T_0) = 58.811 (59.345) kcal/mol at the MRCI level (Table 2). Unfortunately, there are no experimental results in the literature for this state. However, there is no reason to assume that our results for $\tilde{c}^1A_1$ are any less reliable than those for the other states. So, we believe they also are of experimental accuracy.

The leading CASSCF configurations for the $\tilde{c}^1A_1$ state are

$$\left|\tilde{c}^1A_1\right\rangle \sim \left|1a_1^2\,2a_1^2[0.67(3a_1^2) + 0.73(1b_1^2)]1b_2^2\right\rangle$$

The quasilinear character of this state (θ_e = 171.92°, IB = 10.3 cm^{-1}; Table 2) is its unique feature. This structure is easily rationalized after examining its linear limiting configuration ($^1\Sigma_g^+$), which correlates to CH($C^2\Sigma^+$) + H(^{2}S) (Fig. 2). The nature of this state becomes obvious upon considering the following diagram showing the unique way that $CH_2(^1\Sigma_g^+)$ is formed from CH + H:

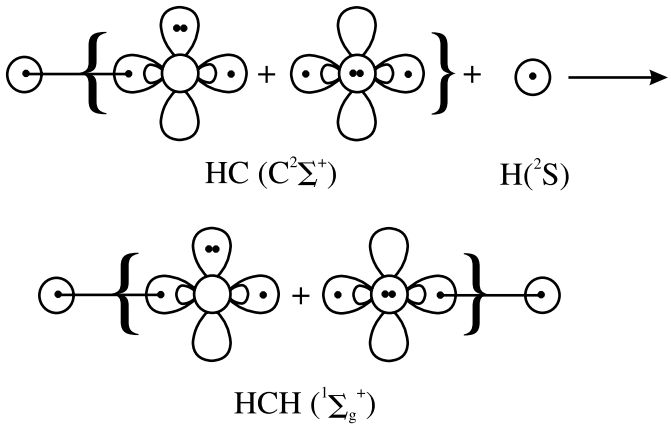

With no other competitive CH state available (126) the final CH_2 state is, indeed, essentially vibrationally linear with an inversion energy barrier that is close to zero.

Conclusions

Using all electron multireference calculations and large basis sets we constructed potential energy curves along the HĈH and CH + H coordinates for the four lowest states of the CH_2 system, namely $\tilde{X}^3B_1$, $\tilde{a}^1A_1$, $\tilde{b}^1B_1$, and $\tilde{c}^1A_1$. Our geometrical results, binding energies, and energy separations are in excellent agreement with existing experimental values.

Taking into account the low-lying states of the CH diatomic molecule ($X^2\Pi$, $a^4\Sigma^-$, $A^2\Delta$, $B^2\Sigma^-$, and $C^2\Sigma^+$), we can rationalize the bonding schemes and geometrical characteristics of the four states of CH_2 examined in this paper. In particular, the large range of inversion barriers to linearity (5.668, 26.355, 2.725, 0.029 kcal/mol, respectively) can be comprehended in terms of the energy splittings among the related states of the CH fragment.

Acknowledgements

This work was performed in part at the Joint Institute for Computational Sciences, University of Tennessee–Oak Ridge National Laboratory. Support was provided by the Distinguished Scientist Program at the University of Tennessee and Oak Ridge National Laboratory. Oak Ridge National Laboratory is managed by UT–Battelle, LLC for the U.S. Department of Energy under Contract No. DE–AC05–00OR22725.

References

1. R.S. Mulliken. Phys. Rev. **41**, 751 (1932).
2. G. Herzberg. Astrophys. J. **96**, 314 (1942).
3. G. Herzberg and J. Shoosmith. Nature (London), **183**, 1801 (1959).
4. J.M. Foster and S.F. Boys. Rev. Mod. Phys. **32**, 305 (1960).
5. G. Herzberg. Proc. R. Soc. London A, **262**, 291 (1961).
6. G. Herzberg. Can J. Phys. **39**, 1511 (1961).
7. G. Herzberg and J.W.C. Johns. Proc. R. Soc. London A, **295**, 107 (1966).
8. J.F. Harrison and L.C. Allen. J. Am. Chem. Soc. **91**, 807 (1969).
9. C.F. Bender and H.F. Schaefer III. J. Am. Chem. Soc. **92**, 4984 (1970).
10. R.A. Bernheim, H.W. Bernard, P.S. Wang, L.S. Wood, and P.S. Skell. J. Chem. Phys. **53**, 1280 (1970).
11. E. Wasserman, W.A. Yager, and V.J. Kuck. Chem. Phys. Lett. **7**, 409 (1970).
12. E. Wasserman, V.J. Kuck, R.S. Hutton, and W.A. Yager. J. Am. Chem. Soc. **92**, 7491 (1970).
13. J.F. Harrison. J. Chem. Phys. **54**, 5413 (1971).
14. J.F. Harrison. J. Am. Chem. Soc. **93**, 4112 (1971).
15. J.F. Harrison. Int. J. Quantum Chem. **5**, 285 (1971).
16. G. Herzberg and J.W.C. Johns. J. Chem. Phys. **54**, 2276 (1971).
17. R.A. Bernheim, H.W. Bernard, P.S. Wang, L.S. Wood, and P.S. Skell. J. Chem. Phys. **54**, 3223 (1971).
18. E. Wasserman, V.J. Kuck, R.S. Hutton, E.D. Anderson, and W.A. Yager. J. Chem. Phys. **54**, 4120 (1971).
19. E. Wasserman, R.S. Hutton, V.J. Kuck, and W.A. Yager. J. Chem. Phys. **55**, 2593 (1971).
20. S.V. O'Neil, H.F. Schaefer III, and C.F. Bender. J. Chem. Phys. **55**, 162 (1971).
21. J.F. Harrison. *In* Carbene chemistry. *Edited by* W. Kirmse. Academic Press, Inc., New York and London. 1971.
22. P.J. Hay, W.J. Hunt, and W.A. Goddard III. Chem. Phys. Lett. **13**, 30 (1972).
23. C.F. Bender, H.F. Schaefer III, D.R. Franceschetti, and L.C. Allen. J. Am. Chem. Soc. **94**, 6888 (1972).
24. D.R. McLaughlin, H.F. Schaefer, and C.F. Bender. Theor. Chim. Acta, **25**, 352 (1972).
25. V. Staemmler. Theor. Chim. Acta, **31**, 49 (1973).
26. J.F. Harrison. J. Chem. Phys. **58**, 3106 (1973).
27. J.F. Harrison. Acc. Chem. Res. **7**, 378 (1974).
28. P.P. Gaspar and G.S. Hammond. *In* Carbenes. *Edited by* R.A. Moss and M. Jones. Wiley, New York. 1975.
29. J.F. Harrison and D.A. Wernette. J. Chem. Phys. **62**, 2918 (1975).
30. R.J. Blint and M.D. Newton. Chem. Phys. Lett. **32**, 178 (1975).
31. A.H. Pakiari and N.C. Handy. Theor. Chim. Acta, **40**, 17 (1975).
32. J.H. Meadows and H.F. Schaefer III. J. Am. Chem. Soc. **98**, 4383 (1976).
33. P.F. Zittel, G.B. Ellison, S.V. O'Neil, E. Herbst, W.C. Lineberger, and W.P. Reinhardt. J. Am. Chem. Soc. **98**, 3731 (1976).
34. R.A. Bernheim, T. Adl, H.W. Benard, A. Songco, P.S. Wang, R. Wang, L.S. Wood, and P.S. Skell. J. Chem. Phys. **64**, 2747 (1976).
35. L.B. Harding and W.A. Goddard III. J. Chem. Phys. **67**, 1777 (1977).
36. R.R. Lucchese and H.F. Schaefer III. J. Am. Chem. Soc. **99**, 6765 (1977).
37. C.W. Bauschlicher, Jr., H.F. Schaefer III, and P.S. Bagus. J. Am. Chem. Soc. **99**, 7106 (1977).
38. B.O. Roos and P.M. Siegbahn. J. Am. Chem. Soc. **99**, 7716 (1977).
39. S. Shih, S.D. Peyerimhoff, R.J. Buenker, and M. Peric. Chem. Phys. Lett. **55**, 206 (1978).
40. C.W. Bauschlicher, Jr. and I. Shavitt. J. Am. Chem. Soc. **100**, 739 (1978).
41. R.K. Lengel and R.N. Zare. J. Am. Chem. Soc. **100**, 7495 (1978).
42. C.W. Bauschlicher, Jr. and D.R. Yarkony. J. Chem. Phys. **69**, 3875 (1978).
43. L.B. Harding and W.A. Goddard III. Chem. Phys. Lett. **55**, 217 (1978).
44. W.T. Borden and E.R. Davidson. Ann. Rev. Phys. Chem. **30**, 125 (1979).
45. C.W. Bauschlicher, Jr. Chem. Phys. Lett. **74**, 273 (1980).
46. E.R. Davidson, D. Feller, and P. Phillips. Chem. Phys. Lett. **76**, 416 (1980).
47. J. Römelt, S.D. Peyerimhoff, and R.J. Buenker. Chem. Phys. **54**, 147 (1981).
48. P.C. Engelking, R.R. Corderman, J.J. Wendoloski, G.B. Ellison, S.V. O'Neil, and W.C. Lineberger. J. Chem. Phys. **74**, 5460 (1981).
49. P. Saxe, H.F. Schaefer III, and N.C. Handy. J. Phys. Chem. **85**, 745 (1981).
50. T.J. Sears, P.R. Bunker, and A.R.W. McKellar. J. Chem. Phys. **75**, 4731 (1981).

51. C.C. Hayden, D.M. Neumark, K. Shobatake, R.K. Sparks, and Y.T. Lee. J. Chem. Phys. **76**, 3607 (1982).
52. T.J. Sears, P.R. Bunker, A.R.W. McKellar, K.M. Evenson, D.A. Jennings, and J.M. Brown. J. Chem. Phys. **77**, 5348 (1982).
53. T.J. Sears, P.R. Bunker, and A.R.W. McKellar. J. Chem. Phys. **77**, 5363 (1982).
54. P. Jensen, P.R. Bunker, and A.R. Hoy. J. Chem. Phys. **77**, 5370 (1982).
55. L.B. Harding. J. Phys. Chem. **87**, 441 (1983).
56. P. Knowles, N.C. Handy, and S. Carter. Mol. Phys. **49**, 681 (1983).
57. H. Petek, D.J. Nesbitt, P.R. Ogilby, and C.B. Moore. J. Phys. Chem. **87**, 5367 (1983).
58. P.R. Bunker, T.J. Sears, A.R.W. McKellar, K.M. Evenson, and F.J. Lovas. J. Chem. Phys. **79**, 1211 (1983).
59. A.R.W. McKellar, C. Yamada, and E. Hirota. J. Chem. Phys. **79**, 1220 (1983).
60. P.R. Bunker and P. Jensen. J. Chem. Phys. **79**, 1224 (1983).
61. A.R.W. McKellar, P.R. Bunker, T.J. Sears, K.M. Evenson, R.J. Saykally, and S.R. Langhoff. J. Chem. Phys. **79**, 5251 (1983).
62. T.J. Sears and P.R. Bunker. J. Chem. Phys. **79**, 5265 (1983).
63. D.G. Leopold, K.K. Murray, and W.C. Lineberger. J. Chem. Phys. **81**, 1048 (1984).
64. S.J. Cole, G.D. Purvis III, and R.J. Bartlett. Chem. Phys. Lett. **113**, 271 (1985).
65. I. Shavitt. Tetrahedron, **41**, 1531 (1985).
66. P.R. Bunker. *In* Comparison of ab initio quantum chemistry with experiment for small molecules. *Edited by* R.J. Bartlett. D. Reidel Publishing Company, Dordrecht, The Netherlands. 1985.
67. W.A. Goddard III. Science (Washington, D.C.), **227**, 917 (1985).
68. D.G. Leopold, K.K. Murray, A.E.S. Miller, and W.C. Lineberger. J. Chem. Phys. **83**, 4849 (1985).
69. P.R. Bunker and T.J. Sears. J. Chem. Phys. **83**, 4866 (1985).
70. H.F. Schaefer III. Science (Washington, D.C.), **231**, 1100 (1986).
71. N.C. Handy, Y. Yamaguchi, and H.F. Schaefer III. J. Chem. Phys. **84**, 4481 (1986).
72. T.J. Sears. J. Chem. Phys. **85**, 3711 (1986).
73. M.D. Marshall and A.R.W. McKellar. J. Chem. Phys. **85**, 3716 (1986).
74. P.R. Bunker, P. Jensen, W.P. Kraemer, and R. Beardsworth. J. Chem. Phys. **85**, 3724 (1986).
75. C.W. Bauschlicher, Jr. and P.R. Taylor. J. Chem. Phys. **85**, 6510 (1986).
76. E.A. Carter and W.A. Goddard III. J. Chem. Phys. **86**, 862 (1987).
77. H. Petek, D.J. Nesbitt, D.C. Darwin, and C.B. Moore. J. Chem. Phys. **86**, 1172 (1987).
78. H. Petek, D.J. Nesbitt, C.B. Moore, F.W. Birss, and D.A. Ramsay. J. Chem. Phys. **86**, 1189 (1987).
79. C.W. Bauschlicher, Jr., S.R. Langhoff, and P.R. Taylor. J. Chem. Phys. **87**, 387 (1987).
80. A.D. McLean, P.R. Bunker, R.M. Escribano, and P. Jensen. J. Chem. Phys. **87**, 2166 (1987).
81. G. Duxbury and Ch. Jungen. Mol. Phys. **63**, 981 (1988).
82. P. Jensen and P.R. Bunker. J. Chem. Phys. **89**, 1327 (1988).
83. W. Xie, A. Ritter, C. Harkin, K. Kasturi, and H.-L. Dai. J. Chem. Phys. **89**, 7033 (1988).
84. D.C. Comeau, I. Shavitt, P. Jensen, and P.R. Bunker. J. Chem. Phys. **90**, 6491 (1989).
85. H. Petek, D.J. Nesbitt, D.C. Darwin, P.R. Ogilby, C.B. Moore, and D.A. Ramsay. J. Chem. Phys. **91**, 6566 (1989).
86. W. Xie, C. Harkin, and H.-L. Dai. J. Chem. Phys. **93**, 4615 (1990).
87. A. Alijah and G. Duxbury. Mol. Phys. **70**, 605 (1990).
88. W.H. Green, Jr., N.C. Handy, P.J. Knowles, and S. Carter. J. Chem. Phys. **94**, 118 (1990).
89. K.K. Irikura and J.W. Hudgens. J. Phys. Chem. **96**, 518 (1992).
90. K.K. Irikura, R.D. Johnson III, and J.W. Hudgens. J. Phys. Chem. **96**, 6131 (1992).
91. I. Garcia-Moreno, E.R. Lovejoy, C.B. Moore, and G. Duxbury. J. Chem. Phys. **98**, 873 (1993).
92. G.V. Hartland, D. Qin, and H.-L. Dai. J. Chem. Phys. **98**, 2469 (1993).
93. I. Garcia-Moreno and C.B. Moore. J. Chem. Phys. **99**, 6429 (1993).
94. L.B. Harding, R. Guadagnini, and G.C. Schatz. J. Phys. Chem. **97**, 5472 (1993).
95. V.J. Barclay, I.P. Hamilton, and P. Jensen. J. Chem. Phys. **99**, 9709 (1993).
96. B.-C. Chang, M. Wu, G.E. Hall, and T.J. Sears. J. Chem. Phys. **101**, 9236 (1994).
97. P. Piecuch, X. Li, and J. Paldus. Chem. Phys. Lett. **230**, 377 (1994).
98. A. Balková and R.J. Bartlett. J. Chem. Phys. **102**, 7116 (1995).
99. (*a*) R.A. Beärda, M.C. van Hemert, and E.F. van Dishoeck. J. Chem. Phys. **97**, 8240 (1992); (*b*) G.-J. Kroes, E.F. van Dishoeck, R.A. Beärda, and M.C. van Hemert. J. Chem. Phys. **99**, 228 (1993); (*c*) R.A. Beärda, G.-J. Kroes, M.C. van Hemert, B. Heumann, R. Schinke, and E.F. van Dishoeck. J. Chem. Phys. **100**, 1113 (1993); (*d*) G.-J. Kroes and M.C. van Hemert. J. Chem. Phys. **100**, 1128 (1994); (*e*) R.A. Beärda, M.C. van Hemert, and E.F. van Dishoeck. J. Chem. Phys. **102**, 8930 (1995).
100. G.V. Hartland, D. Qin, and H.-L. Dai. J. Chem. Phys. **102**, 6641 (1995).
101. D.E. Woon and T.H. Dunning, Jr. J. Chem. Phys. **103**, 4572 (1995).
102. D.R. Yarkony. J. Chem. Phys. **104**, 2932 (1996).
103. Y. Yamaguchi, C.D. Sherrill, and H.F. Schaefer III. J. Phys. Chem. **100**, 7911 (1996).
104. P.R. Bunker, P. Jensen, Y.Yamaguchi, and H.F. Schaefer III. J. Mol. Spectrosc. **179**, 263 (1996).
105. P.R. Bunker, P. Jensen, Y. Yamaguchi, and H.F. Schaefer III. J. Phys. Chem. **100**, 18 088 (1996).
106. Y. Yamaguchi and H.F. Schaefer III. J. Chem. Phys. **106**, 1819 (1997).
107. C.D. Sherrill, T.J. van Huis, Y. Yamaguchi, and H.F. Schaefer III. J. Mol. Struct.: THEOCHEM, **400**, 139 (1997).
108. K.A. Peterson and T.H. Dunning, Jr. J. Chem. Phys. **106**, 4119 (1997).
109. Y. Yamaguchi and H.F. Schaefer III. J. Chem. Phys. **106**, 8753 (1997).
110. Y. Yamaguchi and H.F. Schaefer III. Chem. Phys. **225**, 23 (1997).
111. C.D. Sherrill, M.L. Leininger, T.J. van Huis, and H.F. Schaefer III. J. Chem. Phys. **108**, 1040 (1998).
112. G. Duxbury, A. Alijah, B.D. McDonald, and C. Jungen. J. Chem. Phys. **108**, 2351 (1998).
113. G. Duxbury, B.D. McDonald, M. van Gogh, A. Alijah, C. Jungen, and H. Palivan. J. Chem. Phys. **108**, 2336 (1998).
114. C. Fockenberg, A.J. Marr, T.J. Sears, and B.-C. Chang. J. Mol. Spectrosc. **187**, 119 (1998).

115. A.J. Marr, T.J. Sears, and B.-C. Chang. J. Chem. Phys. **109**, 3431 (1998).
116. D.R. Yarkony. J. Chem. Phys. **109**, 7047 (1998).
117. J.-P. Gu, G. Hirsch, R.J. Buenker, M. Brumm, G. Osmann, P.R. Bunker, and P. Jensen. J. Mol. Struct. **517–518**, 247 (2000).
118. B. Bussery-Honvault, P. Honvault, and J.-M. Launay. J. Chem. Phys. **115**, 10 701 (2001).
119. L. Bañares, F.J. Aoiz, P. Honvault, B. Bussery-Honvault, and J.-M. Launay. J. Chem. Phys. **118**, 565 (2003).
120. J.-S.K. Yu, S.-Y. Chen, and C.-H. Yu. J. Chem. Phys. **118**, 582 (2003).
121. A.G. Császár, M.L. Leininger, and V. Szalay. J. Chem. Phys. **118**, 10 631 (2003).
122. T.H. Dunning, Jr. J. Chem. Phys. **90**, 1007 (1989); A.K. Wilson, T. van Mourik, and T.H. Dunning, Jr. J. Mol. Struct.: THEOCHEM, **388**, 339 (1997); D.E. Woon and T.H. Dunning, Jr. J. Chem. Phys. **100**, 2975 (1994); D.E. Woon and T.H. Dunning, Jr. J. Chem. Phys. **103**, 4572 (1995).
123. K.A. Peterson, D.E. Woon, and T.H. Dunning, Jr. J. Chem. Phys. **100**, 7410 (1994).
124. H. Partridge. J. Chem. Phys. **90**, 1043 (1989).
125. R.D. Amos, A. Bernhardsson, A. Berning, P. Celani, D.L. Cooper, M.J.O. Deegan, A.J. Dobbyn, F. Eckert, C. Hampel, G. Hetzer, P.J. Knowles, T. Korona, R. Lindh, A.W. Lloyd, S.J. McNicholas, F.R. Manby, W. Meyer, M.E. Mura, A. Nicklass, P. Palmieri, R. Pitzer, G. Rauhut, M. Schütz, U. Schumann, H. Stoll, A.J. Stone, R. Tarroni, T. Thorsteinsson, and H.-J. Werner. MOLPRO, version 2002.6 [computer program]. See www.molpro.net.
126. A. Kalemos, A. Mavridis, and A. Metropoulos. J. Chem. Phys. **111**, 9536 (1999).
127. R. Atkinson, D.L. Baulch, R.A. Cox, R.F. Hampson, Jr., J.A. Kerr, M.J. Rossi, and J. Troe. J. Phys. Chem. Ref. Data, **29**, 167 (2000).